Multipolar interband absorption in a semiconductor quantum dot. II. Magnetic dipole enhancement

Jorge R. Zurita-Sánchez and Lukas Novotny

The Institute of Optics, University of Rochester, Rochester, New York 14627

Received February 21, 2002; revised manuscript received June 3, 2002

We derive the magnetic dipole selection rules and the magnetic dipole absorption rate for a spherical semiconductor quantum dot. We find that electric dipole and magnetic dipole transitions are exclusive and therefore can be spectrally distinguished. The magnitudes of electric and magnetic absorption rates are compared for excitation with a strongly focused azimuthally polarized beam. It turns out that spatial optical resolution can be increased by detection of the ratio of magnetic and electric absorption rates. Resolution is limited only by the purity of the laser mode used for excitation. © 2002 Optical Society of America

OCIS codes: 160.4760, 160.6000, 300.6470.

1. INTRODUCTION

Optical spectroscopy of atoms and molecules is concerned mainly with electric dipole transitions, which are usually much stronger than magnetic dipole transitions. An exception is optical spectroscopy based on circular dichroism, which is applied to chiral molecules, that is, molecules that do not possess a center of inversion or a plane of symmetry. Chiral molecules exhibit different photon absorption rates for excitations with left and right circular polarization because of the interference between electric dipole and magnetic dipole transitions.[1] Furthermore, for various kinds of nanostructures (quantum dots, quantum wells, quantum wires) it has been shown that new schemes of optical excitation, such as near-field illumination, may modify the standard selection rules and improve the classical resolution limit (see references cited in Ref. 2). In Ref. 3 Hanewinkel *et al.* calculate the optical response of a quantum dot excited by the field near a tiny aperture. In the near zone of the aperture, the ratio of the magnetic and the electric field ($|\mathbf{B}|/|\mathbf{E}|$) is roughly inversely proportional to the diameter of the aperture; that is, the magnetic field becomes stronger as the diameter is reduced, and, as a consequence, the magnetic dipole absorption rate becomes stronger. However, the authors of Ref. 3 also point out that for a realistic aperture the magnetic dipole response is very small compared with the electric dipole response. Consequently, magnetic dipole transitions can be neglected in aperture-type near-field optical microscopy.

The present paper is a sequel to Ref. 2, which analyzed electric quadrupole transitions in a spherical quantum dot exposed to a strongly confined optical near field. Here we study the response of a quantum dot excited by an azimuthally polarized laser beam. The field of this beam, formed by a superposition of two first-order Hermite–Gaussian laser modes, has the peculiarity that the ratio between the magnetic and the electric field is strongly increased in comparison with the fields of a plane wave ($|\mathbf{B}|/|\mathbf{E}| = 1/c$). As a consequence the magnetic dipole absorption rate of a quantum dot excited by an azimuthally polarized beam can become significant. This paper is aimed at answering the following questions: (1) to what extent are the standard selection rules of a quantum dot affected by an azimuthally polarized laser beam, and (2) can spatial resolution be improved by measuring the ratio between magnetic dipole absorption and electric dipole absorption rates? In our analysis, we consider a spherical quantum dot in the strong confinement limit with *no* Coulomb interaction between hole and electron. Furthermore, we use a semiclassical multipolar formalism to describe the interaction between the quantum dot and the electromagnetic field.

This paper uses the same notation and definitions as Ref. 2, and we occasionally refer to the results in Ref. 2. The organization of this paper is as follows. In Section 2 the magnetic dipole absorption rate is derived. In Section 3 the azimuthally polarized beam is described, and the theory of Section 2 is applied to a spherical quantum dot excited by an azimuthally polarized beam. We use approximated parameters for GaAs to estimate the absorption rate for electric dipole transitions and magnetic dipole transitions. The results are discussed in Section 4, and Section 5 concludes the paper.

2. MAGNETIC DIPOLE ABSORPTION

A. Magnetic Dipole Hamiltonian

We consider a monochromatic magnetic field oscillating with frequency ω

$$\mathbf{B}(\mathbf{r}, t) = \tilde{\mathbf{B}}(\mathbf{r})\exp(-i\omega t) + \text{c.c.} \tag{1}$$

Here $\tilde{\mathbf{B}}(\mathbf{r})$ is the spatial complex amplitude and c.c. denotes complex conjugate. With the origin O set at the center of the quantum dot ($\mathbf{R} = \mathbf{0}$), the magnetic dipole interaction Hamiltonian $\hat{H}^M$ is

 © 2002 Optical Society of America

$$\hat{H}^M = -\mathbf{B}(\mathbf{0}, t) \cdot \frac{e}{2m_o}\hat{\mathbf{r}} \times \hat{\mathbf{p}}, \tag{2}$$

where $\hat{\mathbf{p}}$ is the momentum operator $(-i\hbar\nabla)$ and e and m_o are the charge and the mass of the electron, respectively. In terms of the field operators $\hat{\Psi}^\dagger$ and $\hat{\Psi}$, $\hat{H}^M$ can be expressed as

$$\hat{H}^M = \frac{i\hbar e}{2m_o}\mathbf{B}(\mathbf{0}, t) \cdot \int \hat{\Psi}^\dagger(\mathbf{r})(\mathbf{r} \times \nabla\hat{\Psi})\mathrm{d}^3r. \tag{3}$$

The *interband* transition terms are found by substitution of Eq. (16) of Ref. 2 into the above expression, as

$$\begin{aligned}\hat{H}^M = \frac{i\hbar e}{2m_o}\mathbf{B}(\mathbf{0}, t) \cdot \sum_{nlm}\sum_{rst} \hat{f}^\dagger_{nlm}\hat{g}^\dagger_{rst} \\ \times \frac{1}{V_o}\int u^*_{c,0}(\mathbf{r})\zeta^{e*}_{nlm}(\mathbf{r})\mathbf{r} \\ \times \nabla[u_{v,0}(\mathbf{r})\zeta^h_{rst}(\mathbf{r})]\mathrm{d}^3r + \text{h.c.},\end{aligned} \tag{4}$$

where V_o is the unit cell volume, $u_{v,0}$ ($u_{c,0}$) is the valence (conduction) band Bloch function with corresponding eigenvalue equal to zero, $\zeta^{e(h)}_{nlm}$ is the electron (hole) confinement wave function with quantum numbers (n, l, m), $\hat{f}_{nml}$ ($\hat{g}^\dagger_{nml}$) is the annihilation (creation) operator for an electron (hole) in the conduction (valence) band with envelope function $\zeta^{e(h)}_{nlm}$, and h.c. $(*)$ denotes the Hermitian (complex) conjugate. We calculate the integral of Eq. (4) by decomposing it into a sum of integrals over the volume occupied by individual unit cells. By application of the coordinate transformation $\mathbf{r}' = \mathbf{r} - \mathbf{R}_q$, where $\mathbf{R}_q$ is a translational lattice vector (the lattice remains unchanged when it is translated by $\mathbf{R}_q$), Eq. (5) becomes

$$\begin{aligned}\hat{H}^M = \frac{i\hbar e}{2m_o}\mathbf{B}(\mathbf{0}, t) \cdot \sum_{nlm}\sum_{rst}\sum_q \hat{f}^\dagger_{nlm}\hat{g}^\dagger_{rst} \\ \times \frac{1}{V_o}\int_{V_o} u^*_{c,0}(\mathbf{r}' + \mathbf{R}_q)\zeta^{e*}_{nlm}(\mathbf{r}' + \mathbf{R}_q) \\ \times (\mathbf{r}' + \mathbf{R}_q)\nabla'[u_{v,0}(\mathbf{r}' + \mathbf{R}_q)\zeta^h_{rst}(\mathbf{r}' + \mathbf{R}_q)] \\ \times \mathrm{d}^3r' + \text{h.c.},\end{aligned} \tag{5}$$

where the operator ∇' acts on the coordinates $\mathbf{r}'$. Since $u_{i,0}(\mathbf{r}' + \mathbf{R}_q) = u_{i,0}(\mathbf{r}')$ $(i = c, v)$, and since $\zeta^h_{rst}(\mathbf{r}' + \mathbf{R}_q)$ and $\zeta^e_{nlm}(\mathbf{r}' + \mathbf{R}_q)$ are practically constant in each unit cell volume, Eq. (5) can be approximated as

$$\begin{aligned}\hat{H}^M \approx \frac{i\hbar e}{2m_o}\mathbf{B}(\mathbf{0}, t) \\ \cdot \sum_{nlm}\sum_{rst}\sum_q \hat{f}^\dagger_{nlm}\hat{g}^\dagger_{rst}\mathbf{M}_{cv}\zeta^{e*}_{nlm}(\mathbf{R}_q)\zeta^h_{rst}(\mathbf{R}_q) + \text{h.c.},\end{aligned} \tag{6}$$

where $\mathbf{M}_{cv}$ is defined as

$$\mathbf{M}_{cv} = \frac{1}{V_o}\int_{V_o} u^*_{c,0}(\mathbf{r}')(\mathbf{R}_q + \mathbf{r}') \times \nabla' u_{v,0}(\mathbf{r}')\mathrm{d}^3r'. \tag{7}$$

The term in Eq. (7) that contains $\mathbf{r}' \times \nabla'$ is proportional to the expectation value of the angular momentum. If we assume that the conduction band is s-like and that the valence band is p-like, the expectation value of the angular momentum vanishes. Therefore $\mathbf{M}_{cv}$ becomes

$$\mathbf{M}_{cv} = \mathbf{R}_q \times \mathbf{m}_{cv}, \tag{8}$$

$$\mathbf{m}_{cv} \equiv \frac{1}{V_o}\int_{V_o} u^*_{c,0}(\mathbf{r}')\nabla' u_{v,0}(\mathbf{r}')\mathrm{d}^3r'. \tag{9}$$

Then, with the substitution $\Sigma_q \to \int \mathrm{d}R$, relation (6) becomes

$$\begin{aligned}\hat{H}^M = \frac{i\hbar e}{2m_o}\mathbf{B}(\mathbf{0}, t) \cdot \sum_{nlm}\sum_{rst} \hat{f}^\dagger_{nlm}\hat{g}^\dagger_{rst}\mathbf{D}_{nmlrst} \\ \times \mathbf{m}_{cv} + \text{h.c.},\end{aligned} \tag{10}$$

$$\mathbf{D}_{nmlrst} \equiv \int \zeta^{e*}_{nlm}(\mathbf{R})\,\mathbf{R}\,\zeta^h_{rst}(\mathbf{R})\mathrm{d}^3R. \tag{11}$$

Equation (10) is the final expression for the magnetic dipole Hamiltonian $\hat{H}^M_{\text{int}}$.

B. Transition Rate of the Magnetic Dipole Interaction

From Fermi's golden rule, the magnetic dipole photon absorption rate α^M is

$$\begin{aligned}\alpha^M = \frac{2\pi}{\hbar}\sum_{nlm}\sum_{rst} |\langle nml; rst|\hat{H}^M_{\text{int}}|0\rangle|^2 \\ \times \delta[\hbar\omega - (\mathcal{E}^e_{nl} + \mathcal{E}^h_{rs})],\end{aligned} \tag{12}$$

where $|0\rangle$ is the ground state, $|nlm; rst\rangle$ is the state with one electron with quantum numbers (n, l, m) and one hole with quantum numbers (r, s, t), $\mathcal{E}^e_{nl}$ ($\mathcal{E}^h_{rs}$) is the electron (hole) energy, and δ denotes the Dirac δ function. Substituting Eq. (10) into Eq. (12), we obtain

$$\begin{aligned}\alpha^M = \frac{2\pi}{\hbar}\frac{\hbar^2e^2}{4m_o^2}\sum_{nlm}\sum_{rst} |\tilde{\mathbf{B}}(\mathbf{0}) \cdot (\mathbf{D}_{nmlrst} \times \mathbf{m}_{cv})|^2 \\ \times \delta[\hbar\omega - (\mathcal{E}^e_{nl} + \mathcal{E}^h_{rs})].\end{aligned} \tag{13}$$

It follows from Eq. (13) that the magnetic dipole photon absorption depends on the bulk properties of the material ($\mathbf{m}_{cv}$) *and* the quantum dot properties ($\mathbf{D}_{nmlrst}$). This result is different for the electric dipole, for which the absorption strength only depends on the bulk Bloch wave functions (u_{c0} and u_{v0}).[4] The selection rules for the magnetic dipole transitions are determined by the factor $\mathbf{D}_{nmlrst}$. From Eq. (11) and the confinement wave functions defined in Ref. 2 [see Eq. (31) of Ref. 2], the allowed *interband* magnetic dipole transitions turn out to be

$$m - t = \pm 1, \qquad l - s = \pm 1,$$

or

$$m - t = 0, \qquad l - s = \pm 1.$$

These relationships define the magnetic dipole selection rules, and they coincide with the quadrupole selection rules.[2] It is important to note that transitions that are

magnetic dipole allowed are electric dipole forbidden and vice versa. Therefore electric and magnetic transitions can be spectrally separated.

3. ABSORPTION RATES FOR AZIMUTHALLY POLARIZED COHERENT ILLUMINATION

We consider the excitation of a GaAs quantum dot by a focused azimuthally polarized beam. Such a beam can be generated by the coherent superposition of two orthogonally polarized Hermite–Gaussian (1, 0) laser modes.[5] When focused with an objective with numerical aperture N.A. = $n \sin \theta_{\max}$ (n being the refractive index and $\theta_{\max}$ the angular semiaperture), the electric field in the focal plane reads as[5]

$$\tilde{\mathbf{E}}(\rho, \varphi) = AI_1(\rho)\mathbf{n}_\varphi, \tag{14}$$

where A and $\mathbf{n}_\varphi$ are a constant and the azimuthal unit vector, respectively, and $I_1(\rho)$ is given by

$$I_1(\rho) \equiv \int_0^{\theta_{\max}} f_w(\theta)(\cos\theta)^{3/2}(\sin^2\theta)J_1(k\rho\sin\theta)\mathrm{d}\theta, \tag{15}$$

$$f_w(\theta) \equiv \exp\left(-\frac{1}{f_o^2}\frac{\sin^2\theta}{\sin^2\theta_{\max}}\right), \tag{16}$$

$$f_o \equiv \frac{w_o}{f\sin\theta_{\max}}. \tag{17}$$

Here f is the focal length of the objective, ρ is the cylindrical radial coordinate, w_o is the beam waist radius, $k = n\omega/c$ is the magnitude of the wave vector, f_o is the filling factor of the exit pupil of the objective, and J_n is the nth-order Bessel function (see Fig. 1). The magnetic field turns out to have both radial $[\tilde{B}_\rho(\rho)]$ and axial $[\tilde{B}_z(\rho)]$ components,

$$\tilde{\mathbf{B}}(\rho) = -\frac{An}{c}[I_2(\rho)\mathbf{n}_\rho - 4iI_3(\rho)\mathbf{n}_z], \tag{18}$$

where c is the vacuum speed of light, $\mathbf{n}_\rho$ and $\mathbf{n}_z$ are the radial and longitudinal unit vectors, respectively, and $I_2(\rho)$ and $I_3(\rho)$ are given by

$$I_2(\rho) \equiv \int_0^{\theta_{\max}} f_w(\theta)(\cos\theta)^{1/2}(\sin^2\theta)J_1(k\rho\sin\theta)\mathrm{d}\theta, \tag{19}$$

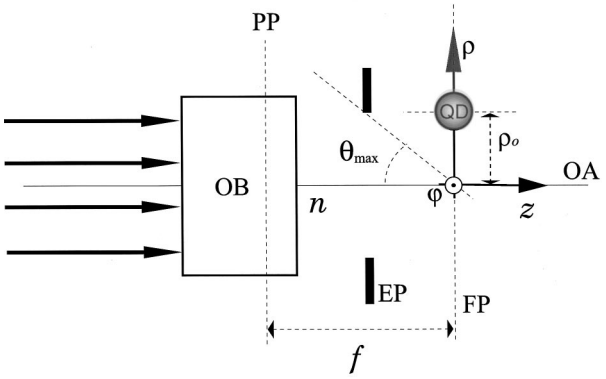

Fig. 1. Excitation of a spherical quantum dot (QD) with a focused azimuthally polarized beam. An objective (OB) with focal distance f [distance between rear principal plane (PP) and focal plane (FP)] and numerical aperture N.A. = $n \sin \theta_{\max}$ focuses an incoming azimuthally polarized beam through an exit pupil (EP) along the optical axis (OA) on the focal plane. The quantum dot is located in the focal plane at $\mathbf{r}_0 = \rho_0\mathbf{n}_\rho$.

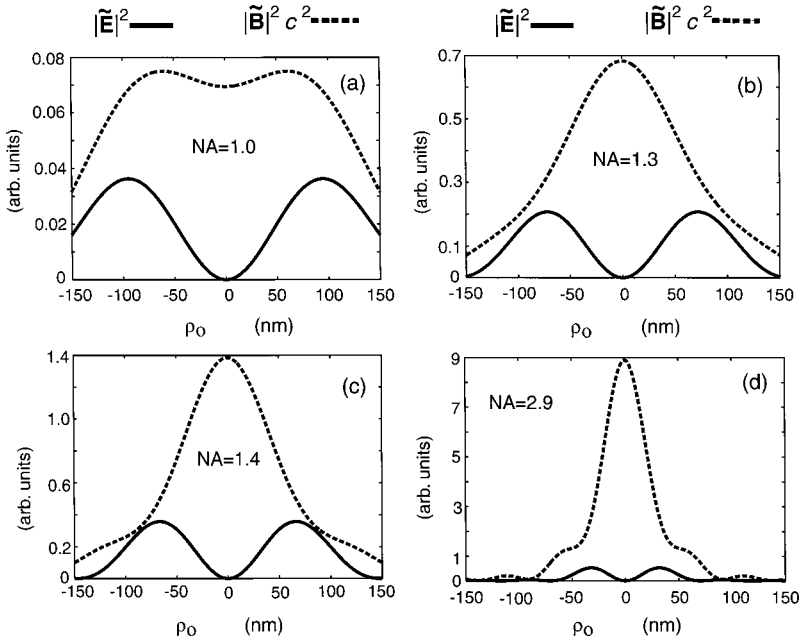

Fig. 2. Electric field $|\tilde{\mathbf{E}}|^2$ (solid curves) and magnetic field $|\tilde{\mathbf{B}}|^2$ (dashed curves) of a focused azimuthally polarized beam evaluated in the focal plane as a function of the radial coordinate ρ_0 for numerical apertures N.A. = 1.0, 1.3, 1.4, 2.9. The electric field is zero at the center, whereas the magnetic field strength increases as the N.A. becomes larger. The wavelength is $\lambda = 532$ nm; the filling factor is $f_0 = 1$.

$$I_3(\rho) \equiv \int_0^{\theta_{\max}} f_w(\theta)(\cos\theta)^{1/2}(\sin^3\theta)J_o(k\rho\sin\theta)\mathrm{d}\theta. \tag{20}$$

Figure 2 shows plots of $|\tilde{\mathbf{E}}(\rho)|^2$ and $|\tilde{\mathbf{B}}(\rho)|^2$ in the focal plane for various numerical apertures. With increasing numerical aperture the fields become better confined, and the strength of the magnetic field increases. It is a characteristic feature of the azimuthally polarized beam that the electric field vanishes on the optical axis. This is analogous to the radially polarized beam for which the magnetic field vanishes on the optical axis.[6]

We now calculate the absorption rates α_E and α_M in a GaAs quantum dot as it is scanned along the radial coordinate ρ in the focal plane ($z = 0$). We use the same Bloch functions as in Ref. 2, which are *approximations* of Bloch functions of GaAs. GaAs has a lattice constant of $d = 0.565$ nm, an effective electron mass of $0.067m_o$, and an effective hole mass of $0.080m_o$.

We take the rotational average of the absorption rate of the lowest-energy allowed electric dipole transition $\langle\alpha^E\rangle$ [see Eq. (37) of Ref. 2]. Also, we calculate the absorption rate for the lowest-energy allowed magnetic dipole transition. This transition creates a hole with quantum numbers (1 1 0) or (1 1 −1) or (1 1 1) (threefold degeneracy) and an electron with quantum numbers (1 0 0). Evaluating the rotational average of Eq. (13) and taking into account the degeneracy of the valence band and the hole energy level, the averaged magnetic dipole absorption rate becomes

$$\langle\alpha^M\rangle = \frac{2\pi}{\hbar}\frac{\hbar^2e^2}{2m_o^2}|\tilde{\mathbf{B}}(\mathbf{0})|^2|\mathbf{D}|^2|\mathbf{m}|^2\delta[\hbar\omega - (\mathcal{E}_{10}^e + \mathcal{E}_{11}^h)], \tag{21}$$

where $|\mathbf{D}|$ and $|\mathbf{m}|$ are given by

$$|\mathbf{D}| = |\mathbf{D}_{100110}| = |\mathbf{D}_{100111}| = |\mathbf{D}_{10011-1}|, \tag{22}$$

$$|\mathbf{m}| = |\mathbf{m}_{cv_1}| = |\mathbf{m}_{cv_2}| = |\mathbf{m}_{cv_3}|. \tag{23}$$

Thus, the ratio $\langle\alpha^M\rangle/\langle\alpha^E\rangle$ becomes

$$\frac{\langle\alpha^M\rangle}{\langle\alpha^E\rangle} = \frac{(2\pi c)^2}{2\lambda^2}|\mathbf{D}|^2\frac{|\tilde{\mathbf{B}}|^2}{|\tilde{\mathbf{E}}|^2}. \tag{24}$$

Evaluating Eq. (31) of Ref. 2 with the corresponding quantum numbers gives $|\mathbf{D}| \approx 0.3a$. In Eq. (24) we used the same wavelength λ for the electric and the magnetic dipole transitions. This is just an approximation, since we determined previously that the electric and magnetic transitions are spectrally different. However, the separation between the two transitions is small (<50 nm), and the error induced by using a single wavelength is not significant.

4. QUANTUM DOT EXCITED BY AN AZIMUTHALLY POLARIZED BEAM

We consider the optical response of a quantum dot with radii of 5 and 10 nm excited by an azimuthally polarized beam. The magnetic absorption rate $\langle\alpha_M\rangle$ depends on $|\tilde{\mathbf{B}}|^2$ and is strongest at the focus of the beam. The dependence of $\langle\alpha_M\rangle$ on the radial coordinate ρ is similar to an Airy function. The width of this response function, *i.e.*, the resolution, depends on the numerical aperture (see Fig. 2). For N.A. = 2.9, the spatial resolution is roughly 100 nm. However, if we simultaneously measure the electric dipole absorption rate $\langle\alpha_E\rangle$, the ratio $\langle\alpha_M\rangle/\langle\alpha_E\rangle$ allows us to drastically increase the spatial resolution.

In Fig. 3, we plot the ratio of electric dipole and magnetic dipole absorption rates ($\langle\alpha_E\rangle/\langle\alpha_M\rangle$) as a function of the radial distance ρ_0 of a quantum dot located in the focal plane. We consider three different numerical apertures. We notice that the ratio $\langle\alpha_E\rangle/\langle\alpha_M\rangle$ is mostly smaller than the ratio that is achieved with pure plane-wave excitation (solid curve). Also, there are intervals for which the ratio becomes smaller than one. These are the regions in which the magnetic dipole absorption rate is larger than the electric dipole absorption rate. The ratio $\langle\alpha_E\rangle/\langle\alpha_M\rangle$ is inversely proportional to the square of the quantum dot radius, as is seen by comparing the scale of the left and the right vertical axes of Fig. 3. Figure 4 shows an enlarged plot of the inverse ratio ($\langle\alpha_M\rangle/\langle\alpha_E\rangle$). At $\rho_0 = 0$, the magnitude of the electric field is zero; therefore the inverse ratio tends to infinity ($\langle\alpha_M\rangle/\langle\alpha_E\rangle \rightarrow \infty$). The width of the plot is independent of the numerical aperture of the objective, although an objective with larger N.A. will provide a better signal-to-noise ratio. Also, the width of the plot depends on the radius of the quantum dot as shown in Fig. 4. For a quantum dot with radius of $a = 5$ nm the width is ~4 nm, and for a quantum dot with a radius of $a = 10$ nm the width is approximately 8 nm. Thus we find that measuring the ratio of the magnetic dipole and the electric dipole absorption rates can enhance the lateral resolution significantly. The resolution is limited only by the signal-to-noise ratio, *i.e.*, by the quality of the azimuthally polarized beam. A mode conversion scheme that provides good mode purity is therefore crucial.

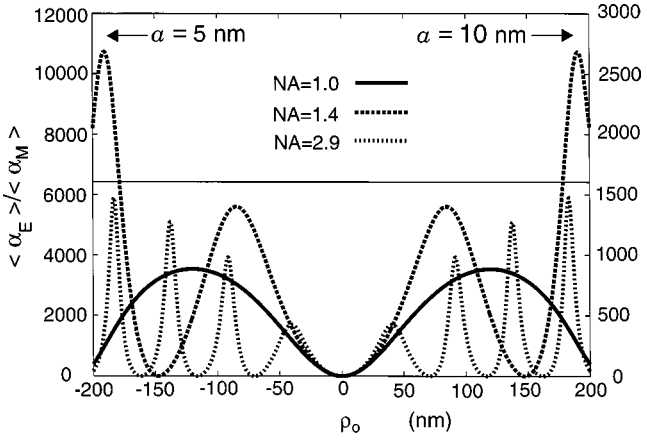

Fig. 3. Ratio of the magnetic dipole and electric dipole absorption rates ($\langle\alpha_E\rangle/\langle\alpha_M\rangle$) as a function of the radial coordinate ρ_0 of the quantum dot. The left (right) vertical axis corresponds to quantum dot radius $a = 5$ nm ($a = 10$ nm). The ratio corresponding to plane-wave excitation is indicated by the horizontal line. λ=532 nm, $fo = 1$.

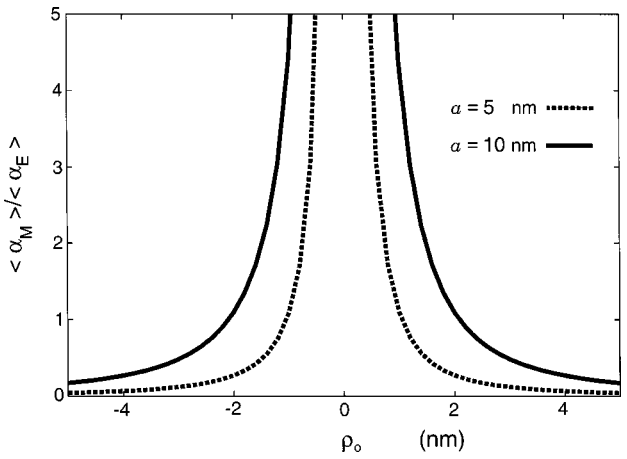

Fig. 4. Inverse ratio ($\langle \alpha_M \rangle / \langle \alpha_E \rangle$) as a function of the radial coordinate ρ_0 of a quantum dot with $a = 5$ nm and $a = 10$ nm. In a length interval of a few nanometers, the magnetic dipole absorption rate is stronger than the electric dipole absorption rate. The ratio is largely independent of N.A., but a large N.A. is required for a good signal-to-noise ratio. $\lambda = 532$ nm, $f_0 = 1$.

5. CONCLUSION

We derived the magnetic dipole absorption rate and the selection rules for a quantum dot in the strong confinement limit. We have neglected the Coulomb interaction between hole and electron, and we assumed that the valence band has a *p*-like character and the conduction band an *s*-like character. Unlike the electric dipole absorption strength, which depends only on bulk Bloch functions, the magnetic absorption strength also depends on the confinement functions. The selection rules for electric dipole and magnetic dipole transitions are different, which allows them to be probed independently from each other. Although we assumed a simple model for the quantum dot, the calculated magnetic dipole and electric dipole absorption rates should coincide with the corresponding values of a realistic quantum dot to within an order of magnitude.

We have analyzed the magnetic dipole interaction in a spherical semiconductor quantum dot excited by an azumithally polarized beam. It is found that an arbitrary resolution can be achieved by measurement of the ratio of magnetic dipole absorption and electric dipole absorption. The resolution is limited only by the mode purity of the excitation beam. For a given mode purity, the resolution depends on the quantum dot size. This method can also be applied to other quantum systems, such as an atom. However, for an atom the magnetic dipole absorption rate is roughly 2 orders of magnitude weaker than the magnetic dipole absorption rate for a quantum dot, since the magnetic absorption rate is proportional to the square of the length of the structure.

ACKNOWLEDGMENTS

We thank Stephan W. Koch and Andreas Knorr for valuable input to this work. This research was supported by the U.S. Department of Energy through grant DE-FG02-01ER15204 and by a Fulbright-CONACyT Fellowship (JZ-S).

REFERENCES

1. D. P. Craig and T. Thirunamachandran, *Molecular Quantum Electrodynamics* (Dover, Mineola, New York, 1998).
2. J. R. Zurita-Sánchez and L. Novotny, "Multipolar interband absorption in a semiconductor. I. Electric quadrupole enhancement," J. Opt. Soc. Am. B **19**, 1355–1362 (2002).
3. B. Hanewinkel, A. Knorr, P. Thomas, and S. W. Koch, "Optical near-field response of semiconductor quantum dots," Phys. Rev. B **55**, 13715–13725 (1997).
4. H. Haug and S. W. Koch, *Quantum Theory of the Optical and Electronic Properties of Semiconductors* (World Scientific, Singapore, 1993).
5. K. S. Youngworth and T. G. Brown, "Focusing of high numerical aperture cylindrical vector beams," Opt. Express **7**, 77–87 (2000).
6. L. Novotny, M. R. Beversluis, K. S. Youngworth, and T. G. Brown, "Longitudinal field modes probed by single molecules," Phys. Rev. Lett. **86**, 5251–5254 (2001).